



# Humidity sensing behaviors of graphene oxide-silicon bi-layer flexible structure

Yao Yao, Xiangdong Chen\*, Huihui Guo, Zuquan Wu, Xiaoyu Li

School of Information Science and Technology, Southwest Jiaotong University, Chengdu 610031, Sichuan, China

## ARTICLE INFO

### Article history:

Received 17 August 2011  
 Received in revised form  
 22 November 2011  
 Accepted 5 December 2011  
 Available online 13 December 2011

### Keywords:

Graphene oxide  
 Silicon flexible microbridge  
 Humidity sensor  
 Bi-layer structure

## ABSTRACT

In this work, we present an approach to use graphene oxide-silicon bi-layer flexible structure as stress-based humidity sensors. By the spin-coating method, graphene oxide thin films were deposited onto silicon microbridge as a humidity sensing layer. Upon expose to humid environment, graphene oxide thin films swells and leads to the bending of silicon membrane. Then, the full piezoresistive Wheatstone-bridge embedded in silicon microbridge was used to transform the deformation into a measurable output voltage. The humidity sensing properties of the bi-layer flexible structure, such as sensitivity, repeatability, humidity hysteresis, response and recovery, were investigated in the wide relative humidity range of 10–98%. The test results show that graphene oxide-silicon bi-layer flexible structure exhibits high humidity sensitivity, good repeatability, small humidity hysteresis and clear and fast response–recovery. Moreover, the dependence of the thin films thickness of graphene oxide on the response properties was also examined. At last, the humidity sensing mechanism of the proposed bi-layer structure was discussed in detail.

© 2011 Published by Elsevier B.V. All rights reserved.

## 1. Introduction

The ability to monitor and control humidity level plays an important role in industry and environmental fields. In the past years, many efforts have been made to develop high performance (i.e. large sensitivity, fast response and recovery, small humidity hysteresis) humidity sensors. Various transduction techniques, such as capacitive [1,2], resistive [3], acoustic [4,5], optical [6] and mechanical [7,8], have been adopted for the design of humidity sensor. Recently, integrated micro- and nano-electro-mechanical system (MEMS/NEMS) devices have been used for a wide range of sensing applications due to their high sensitivity, small size, low cost and capability of compatibility with the integrated circuit (IC) process. Up to now, two major types of silicon MEMS structures, including microbridge [7] and microcantilever [8–10], have been used to develop stress-based humidity sensor by coating humidity sensing material on silicon microstructure. The humidity response behavior of this bi-layer structure is basically analogous to a classical bimorph. The swelling of sensing thin films due to water adsorption results in the deflection of silicon microstructure, integrated piezoelectric or piezoresistive sensing elements was used to transform this deformation into electrical signal. It is worthy of note that these stress-based sensors exhibit the advantages of good reliability and long-term stability under harsh condition as a result of

the intrinsic separation between the mechanical and the electrical elements [7].

For stress-based humidity sensors, the sensing materials actually serve as a humidity-induced mechanical actuator, which play a dominant role in the performance of sensor. In the past, many kinds of ‘polymer-like’ bulk materials, such as polyimide [7], tert-butylcalix[6]arene (TBC6A) [8], gelatin [9], plasma-polymerized methacrylonitrile (PP-MAN) [10], have been studied as strain-type humidity sensing layer. Over the past two decades, nanostructure carbonaceous materials, such as one-dimensional carbon nanotubes (CNT) and zero-dimensional fullerenes (C<sub>60</sub>), have shown a great candidate for gas/humidity sensor application. Compared to polymer-like materials, the nano-carbonaceous materials offer many advantages, such as higher mechanical stiffness, larger surface to volume ratio, and better stability. As a two-dimensional nano-carbon material, graphene (e.g. one thin carbon atom sheet) have attracted increasing attentions in recent years due to its outstanding electrical, thermal, and mechanical properties since the first isolation by Geim and colleagues [11]. These desirable properties have motivated extensive studies on the practical applications of graphene, such as nanoelectronics, chemical sensors and solar cells. To date, graphene based materials have been employed as gas sensing by making use of the change in electrical property of graphene upon exposure to the relevant gas [12–14]. Besides the excellent electrical property for electronics and sensor application, the unique mechanical property of graphene based materials makes it become a considerable candidate for strain actuator.

Graphene oxide (GO), one important derivative of graphene, has also received intensive attentions in many fields ranging from

\* Corresponding author. Tel.: +86 28 87601714; fax: +86 28 87601714.  
 E-mail address: [xdchen@home.swjtu.edu.cn](mailto:xdchen@home.swjtu.edu.cn) (X. Chen).

electronics [15,16] to sensors [17]. More recently, interesting works have reported that the large-scale structural and mechanical properties of GO are strongly affected by atmospheric water vapor [18–20]. It is suggested that water molecules can easily enter into carbon interlayer and form H-bonding networks between water molecules and GO sheet. Park shown that the bi-layer structure which consists of a layer of crisscrossed multi-walled carbon nanotubes (MWCNTs) and a layer of GO platelets exhibited humidity dependent actuation (swelling and shrinking) behaviors [21]. In additional, the deformation of the bi-layer structure is reversible according to the uptake or release of water molecules. The humidity-dependent deformation of GO layer is a very interesting finding, which provide a potential candidate for developing stress-based humidity sensor by combining with MEMS/NEMS technology.

The present work is motivated to investigate the humidity sensing properties of GO-silicon bi-layer flexible structure. By the spin-coating method, GO thin films were deposited onto silicon-based microbridge as a humidity sensing layer. Piezoresistive sensing elements, arranged in full Wheatstone-bridge circuit configuration, were used to measure the swelling of GO induced deflection of silicon microbridge. The test results show that GO-silicon bi-layer flexible structure exhibits high humidity sensitivity, good repeatability, small humidity hysteresis and clear and fast response–recovery.

## 2. Experimental

### 2.1. Fabrication of GO-silicon bi-layer structure

Graphite oxide was synthesized by the oxidative treatment of natural graphite using a modified Hummers method [22]. Subsequently, exfoliation of graphite oxide to single-layered GO sheets was achieved by ultrasonication of graphite oxide dispersion (1 mg/ml) for 1 h. The obtained brown dispersion was centrifugated at 4000 r.p.m. for 2 h to remove any unexfoliated graphite oxide. Then the aqueous suspensions of GO was obtained as a coating solution.

Silicon-based microbridge was fabricated using a standard MEMS process. Anisotropic KOH etching technology was used to generate the microbridge structure (e.g. a thinner silicon membrane) from the back of N-type silicon substrate. The silicon membrane thickness is approximately 20  $\mu\text{m}$ . A layer of silicon nitride which acts as passivation layer was deposited on silicon crystal. Four piezoresistors, arranged in full Wheatstone-bridge circuit configuration, were embedded in the silicon microbridge. Variation in surface stress would cause the bending of the silicon microbridge, and change the resistance values of four piezoresistors. Hence, the full piezoresistive Wheatstone-bridge unbalance and produce a differential output voltage as follow:

$$V_{out} = \frac{V_{in}}{4} \left( \frac{\Delta R_1}{R_1} - \frac{\Delta R_2}{R_2} + \frac{\Delta R_3}{R_3} - \frac{\Delta R_4}{R_4} \right) \quad (1)$$

where  $V_{in}$  is the operation voltage,  $R_i$  is the resistance value of the zero-stress piezoresistor,  $\Delta R_i$  is the change of piezoresistor.

GO dispersion was applied on the silicon microbridge by a spin-coating method. In order to obtain uniform continuous GO thin films,  $\text{N}_2$  gas was used to blow to the chip for accelerating the evaporation of water during the process of spin-coating.

### 2.2. Apparatus

A schematic diagram of the experimental setup is shown in Fig. 1. A temperature and humidity generator was used to generate the required water vapor concentration at a fixed temperature. A commercial humidity–temperature probe (Rotronic, HygroClip

HC2-IC302, Switzerland) was used to calibrate the obtained humidity level and temperature. A DC power supply (Agilent, E3631A, USA) was used to provide the operate voltage (5 V) for sensor. The output measurements of sensor were achieved by a digital multimeter (Agilent, 34410A, USA), which was connected to PC through USB interface. Atomic force microscope (Benyuan, CSPM5500, China) was used to measure the thin films thicknesses of GO. The surface morphology of GO thin films deposited on silicon microstructure was examined by a scanning electron microscope (S-3400N, Hitachi Ltd., Japan).

## 3. Results and discussion

Fig. 2(a) shows the chemical structure of graphene oxide. It can be seen that many oxygen functional groups, such as hydroxyl and epoxy groups attached above and below the basal plane and carboxylic acid groups bound to the edges. The schematic illustration of as-fabricated humidity sensor based on graphene oxide thin films is shown in Fig. 2(b). Many GO sheets stacked together on the silicon microbridge in the form of thin films. Fig. 2(c) plots the full piezoresistive Wheatstone-bridge circuit embedded in the silicon microbridge. The operate voltage of the sensor was 5 V. Fig. 2(d) shows the typical SEM image of GO thin films deposited on silicon membrane. It can be obviously seen that the resultant thin films has an inherent layered structure. For humidity sensing measurement, the response of the sensors as a function of relative humidity (RH) was achieved by inserting the sensors to the chamber of temperature and humidity generator. The temperature of the chamber was controlled at 25  $^\circ\text{C}$  without special representation.

### 3.1. Humidity sensing response

Fig. 3(a) shows the typical humidity sensing response of the sensors to various humidity levels ranging from 10% to 98% RH. The output voltage of the sensor without GO thin films did not demonstrate any obvious change. In contrast, we can find that the output voltage of GO-silicon bi-layer structure with 65-nm-thick GO thin films proportionally increased with increasing the humidity level. Here we define the detection sensitivity as the ratio of the change in output voltage to the change in RH ( $\Delta V/\Delta\text{RH}$ ). The sensitivity of the sensor was 28.02  $\mu\text{V}/\% \text{RH}$ , indicating that the high sensitivity was obtained [23]. Next, the sensor's response curve ranging from 10% RH to 98% RH was fitted and the linear regression coefficient was 0.986. To learn the humidity response repeatability of the sensor, we tested the response of sensor to the humidity variation ranging from 10% RH to 98% RH three times under the same experimental conditions. The test results are shown in Fig. 3(b). We can see that the mainly voltage output difference were occurred at high RH range. Here, we define the repeatable error as the ratio of maximum voltage output deviation to full scale voltage output value, the maximum repeatable error was  $\pm 1.2\%$ .

In additional, the humidity hysteresis characteristic of GO thin film coated sensor was also examined by increasing the RH from 10% to 98% for water molecules absorption and then decreasing back to 10% for water molecules desorption. The test result was shown in Fig. 4. It was found that the RH-decreasing response curve of the sensor slightly lagged behind its RH-increasing response curve. The humidity hysteresis mainly occurred at high RH range. The maximum hysteresis was  $\sim 3\%$  RH occurred at 90% RH.

### 3.2. Dynamic response and recovery

Meanwhile, the response and recovery behavior of GO-silicon bi-layer structure was also tested by applying a humidity pulse between laboratory atmosphere ( $\sim 45\%$  RH) and 98% RH to the sensor. Fig. 5 illustrates the time-dependent response and recovery

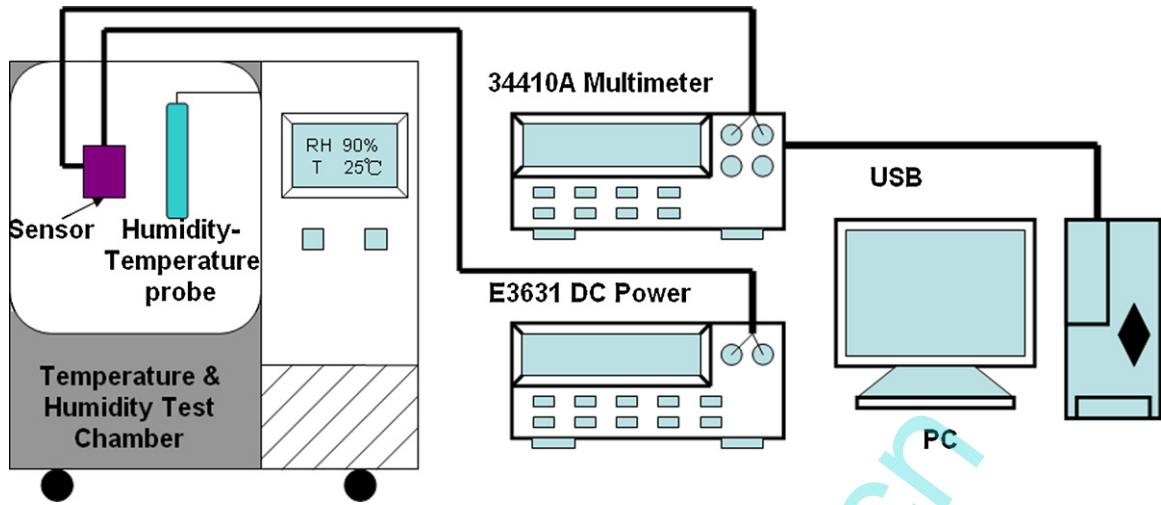


Fig. 1. Schematic diagram of humidity sensing experimental setup.

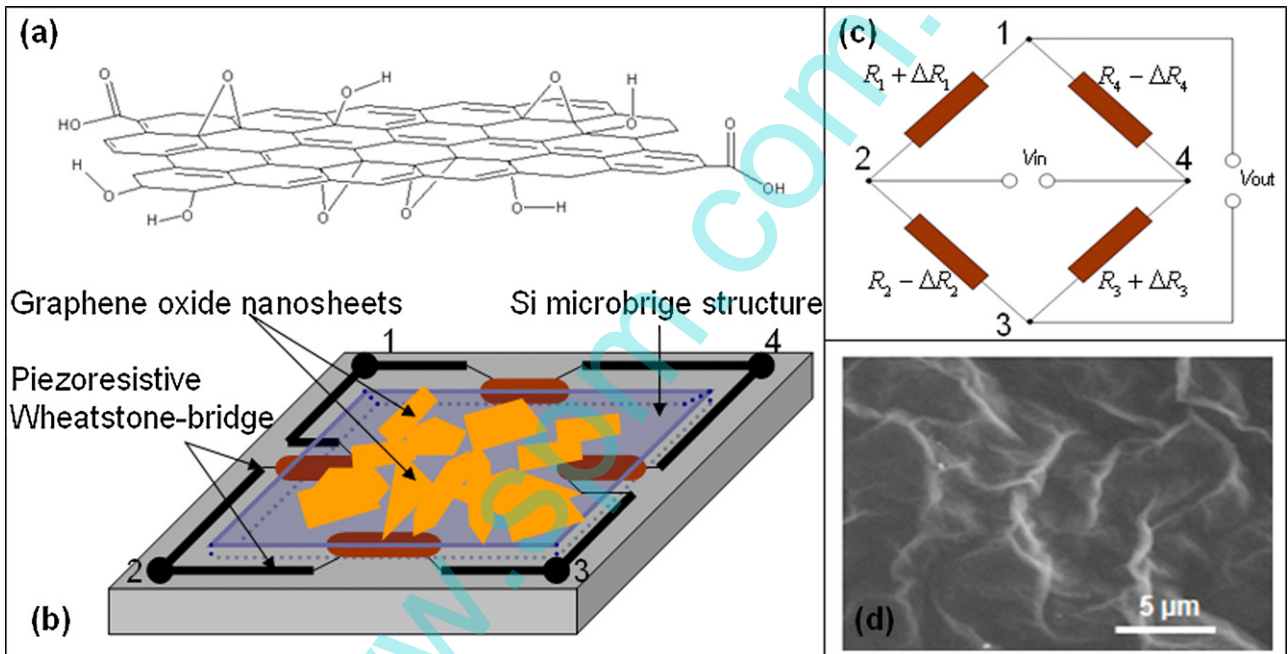


Fig. 2. (a) Chemical structure of graphene oxide; (b) schematic figure of graphene oxide-silicon bi-layer structure; (c) piezoresistive Wheatstone-bridge circuit; (d) typical SEM image of graphene oxide thin films.

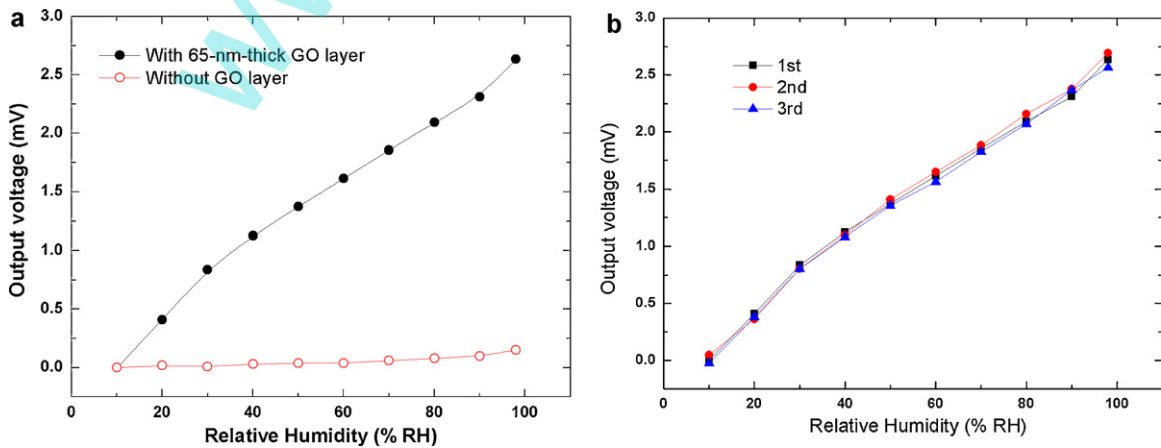


Fig. 3. (a) Typical response curves of sensor with 65-nm-thick GO layer and without GO layer for various RH levels. (b) Repeatability of the sensor with 65-nm-thick GO layer.

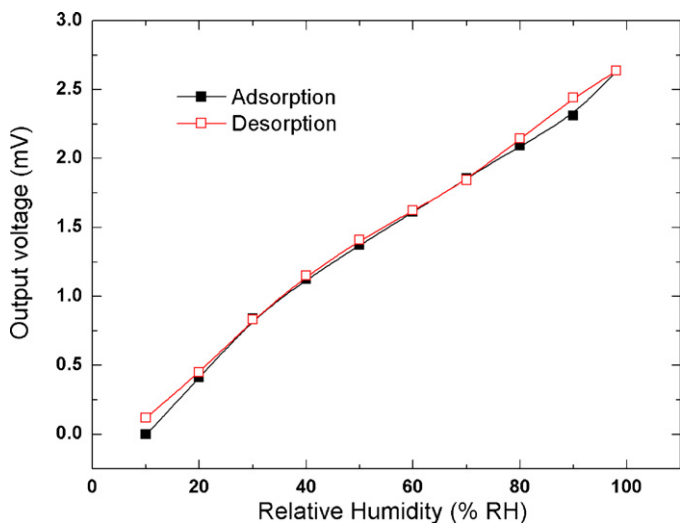


Fig. 4. Humidity hysteresis curves of the sensor with 65-nm-thick GO layer.

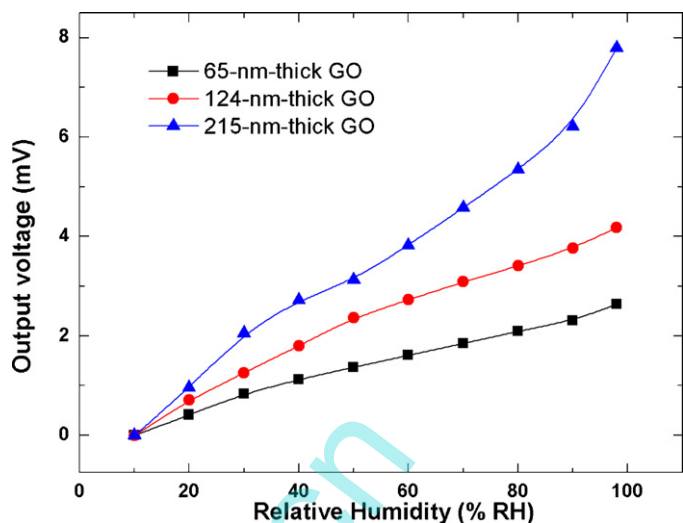


Fig. 6. Humidity response curves of the sensors with different thin films thicknesses.

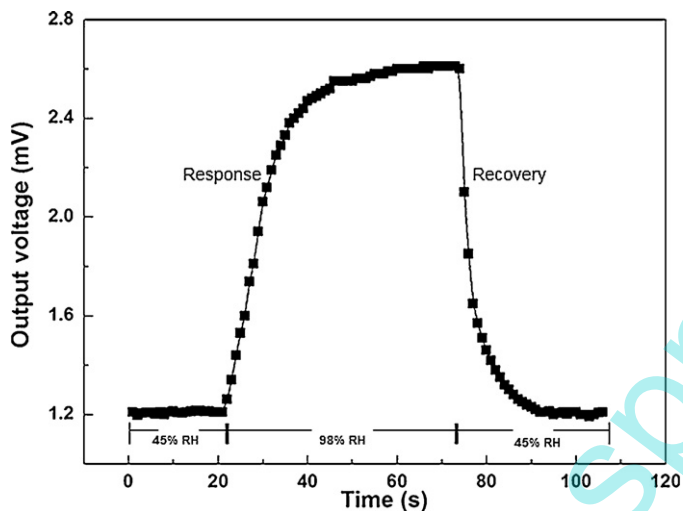


Fig. 5. Time-dependent response and recovery curve of the sensor with 65-nm-thick GO layer to a relative humidity pulse between 45% and 98% RH.

curve of the sensor with 65-nm-thick GO layer. In this experiment, the sensor was firstly exposed to laboratory atmosphere and its stable output in the initial stage was recorded as a baseline. Next, the sensor was put into chamber with 98% RH for the uptake of water molecules until equilibrium is attained. Finally, the sensor was exposed to laboratory atmosphere again for the release of water molecules. As indicated by Fig. 5, the measured response time and recovery time (defined as the time reached 90% of the final steady voltage value) were 19 s and 10 s, respectively. It indicated that the sensor shows a clear and fast response–recovery behavior for humidity sensing [3–5].

### 3.3. The dependence of the thin films thickness of GO on response property

In addition, in order to learn the dependence of the GO thin films thickness on response properties of the sensors, such as sensitivity and linearity, different thicknesses of GO thin films were deposited on silicon microbridge for testing. By adjusting the number of spin-coating cycles, we obtained the other two samples with 124-nm- and 215-nm-thick GO thin films. Fig. 6 shows the typical response versus RH for the sensors. Fig. 7 shows the values of

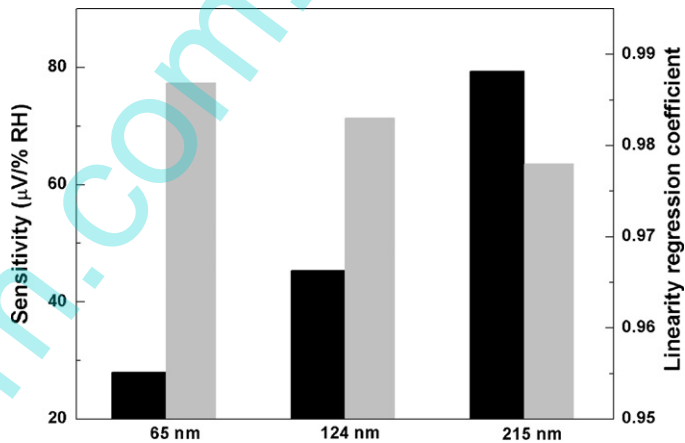


Fig. 7. The sensitivity values (black) and linear regression coefficients (gray) of the sensors with different thin films thicknesses.

sensitivity and linear regression coefficient for the three sensors. As we expected, the thin films thickness of GO has an obvious effect on the response properties of sensor. It can be seen that the sensitivity increased with increasing the thickness of GO thin films. For example, the sensitivity of the sensor with 215-nm-thick GO thin films was  $79.3 \mu\text{V}/\% \text{RH}$ , which was nearly three times greater than that of the sensor with 65-nm-thick GO thin films. Hence, this result suggested that the sensitivity could be tuned by adjusting the thin films thickness of GO. However, we also noted that the linear regression coefficient shown a slight decrease with the increase in the thin films thickness. Therefore, the suitable balance between sensitivity and linearity should be considered in the sensor design.

### 3.4. Discussion

The schematic illustration of humidity sensing response mechanism of GO-silicon bi-layer structure is shown in Fig. 8. Because the electrical interaction between GO layer and piezoresistors was inherently prevented by the passivation layer (silicon nitride), the changes in electrical properties of GO thin films do not influence the humidity response of GO-silicon structure. So, it is believed that the humidity response of the GO-silicon bi-layer structure is attributed to humidity-induced deformation of GO. Since GO contains many oxygen functional groups, such as hydroxyl and epoxy groups attached above and below the basal plane and

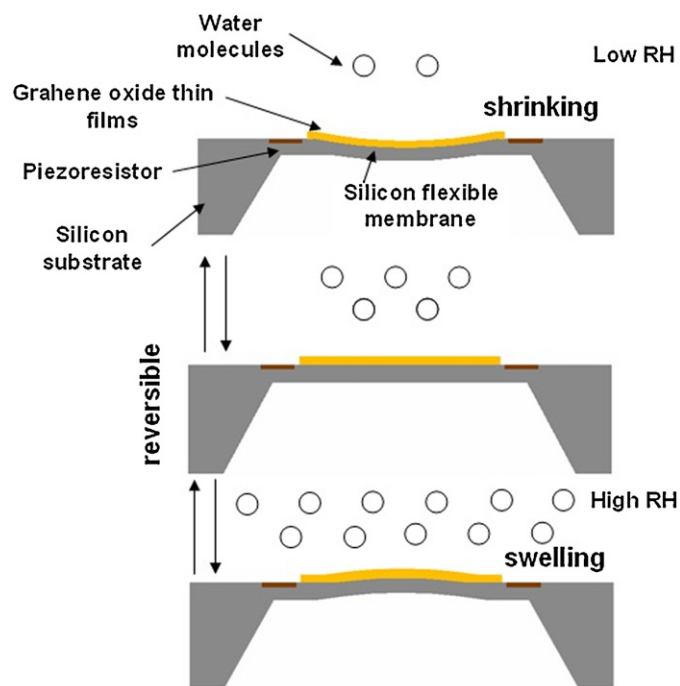


Fig. 8. Schematic illustration of humidity sensing mechanism of graphene oxide thin film coated piezoresistive silicon membrane.

carboxylic acid groups bound to the edges, these oxygen-rich groups makes GO exhibit strongly hydrophilic [24], thus GO can facilitate capture water molecules from external environment. When exposure the bi-layer structure to humid environment, water molecules enter into GO interlayer and form clusters between H-bonding from water molecule and hydroxyl and epoxy groups from GO layer. This process led to an increase in interlayer distance of GO sheets (i.e. swelling of GO thin films) [20]. Consequently, the surface stresses induced by interlayer expansion can apply on the contact surface of silicon microbridge, resulting in the bending of silicon microbridge. Through the full piezoresistive Wheatstone-bridge, this mechanical deformation can be transformed to output voltage. In contrast, in dry environment, the water molecules desorption decreases the interlayer distance of GO sheets (i.e. shrinking of GO thin films), the strain was gradually released and the bending of silicon microbridge was simultaneously recovered.

Thanks to the large swelling property of GO [18], the obtained GO-silicon bi-layer structure exhibits a high humidity sensitivity. Additionally, the degree of GO swelling depends largely on humidity level and the deformation of GO layer exhibits reversible characteristic. Thus, the obtained GO-silicon bi-layer structure shows a small humidity hysteresis property during humidity cycling measurement (see Fig. 4). In Fig. 5, the observed fast response and recovery property of the sensor may be attributed to hydrophilic and thin layer structure properties of GO. On one hand, the hydrophilic property makes GO capture water molecules easily, leading to a fast response. On the other hand, the thin layer structure facilitates the release of water molecules from GO layer for reaching dynamic equilibrium between external humidity level and internal water content [25]. Hence, a clear and fast recovery of sensor can be obtained. Next, we attempt a possible interpretation of the dependence of the thin films thickness of GO on sensor response properties. The sensor with a thicker GO layer shown a larger sensitivity as shown in Fig. 5, this is mainly due to the water adsorption sites, such as hydroxyl and epoxy groups, increased with increasing the thin films thickness. More water molecules enter into GO interlayer, resulting in more

hydrogen-bonded clusters formation. As a result, a larger surface stress induced by swelling of GO layer leads to a larger response sensitivity of sensor.

#### 4. Conclusion

In summary, we have demonstrated that GO-silicon bi-layer structure can be successfully utilized in humidity sensing detection. The as-fabricated structures exhibited excellent humidity sensitivity (the maximum sensitivity reaches  $79.3 \mu\text{V}/\%RH$ ) in a wide detection range of 10–98% RH. Also, it was found that the humidity sensitivity of the bi-layer structure can be enhanced by increasing the thickness of GO thin films. For example, the sensitivity of the sensor with 215-nm-thick GO thin films was nearly three times greater than that of the sensor with 65-nm-thick GO thin films. Finally, the humidity sensing response mechanism of GO thin film coated piezoresistive silicon membrane was discussed in detail. It is suggested that the humidity response of the GO-silicon bi-layer structure is attributed to humidity-induced deformation of GO. This approach provides the advantages of simply structure, low cost and easy integrate in the design of MEMS/NEMS multi-informations sensing sensor.

#### Acknowledgements

The authors wish to thank Professor B.Q. Zeng (School of Physical Electronics, University of Electronic Science and Technology of China) for the help with materials preparation. Supports of this work from National Scientific Foundation of China (No. 60871024) and the Opening Project of State key Laboratory of Electronic Thin Films and Integrated Devices (No. KFJ200915) are acknowledged.

#### References

- [1] P.J. Schubert, J.H. Nevin, A polyimide-based capacitive humidity sensor, *IEEE Trans. Electron. Devices* 32 (1985) 1220–1223.
- [2] G. Sberveglieria, G. Rinchettia, S. Groppellia, G. Faglia, Capacitive humidity sensor with controlled performances, based on porous  $\text{Al}_2\text{O}_3$  thin film grown on  $\text{SiO}_2$ -Si substrate, *Sens. Actuator B* 19 (1994) 551–553.
- [3] Y. Zhang, K. Yu, D. Jiang, Z. Zhu, H. Geng, L. Luo, Zinc oxide nanorod and nanowire for humidity sensor, *Appl. Surf. Sci.* 242 (2005) 212–217.
- [4] X.F. Wang, B. Ding, J.Y. Yu, M. Wang, F. Pan, A highly sensitive humidity sensor based on a nanofibrous membrane coated quartz crystal microbalance, *Nanotechnology* 21 (2010) 055502.
- [5] M. Penza, V.I. Anisimkin, Surface acoustic wave humidity sensor using polyvinyl-alcohol film, *Sens. Actuator A* 76 (1999) 162–166.
- [6] F. Arregui, Y.J. Liu, I. Matias, R. Claus, Optical fiber humidity sensor using a nano Fabry–Perot cavity formed by the ionic self-assembly method, *Sens. Actuator B* 59 (1999) 54–59.
- [7] G. Gerlach, K. Sager, A piezoresistive humidity sensor, *Sens. Actuator A* 43 (1994) 181–184.
- [8] D.R. Southworth, L.M. Bellan, Y. Linzon, H.G. Craighead, J.M. Parpia, Stress-based vapor sensing using resonant microbridges, *Appl. Phys. Lett.* 96 (2010) 163503.
- [9] G.Y. Chen, T. Thundat, E.A. Wachter, R.J. Warmack, Adsorption-induced surface stress and its effects on resonance frequency of microcantilevers, *J. Appl. Phys.* 77 (1995) 3618–3622.
- [10] S. Singamaneni, M.E. McConney, M.C. LeMieux, H. Jiang, J.O. Enlow, T.J. Bunning, R.R. Naik, V.V. Tsukruk, Polymer–silicon flexible structures for fast chemical vapor detection, *Adv. Mater.* 19 (2007) 4248–4255.
- [11] K.S. Novoselov, A.K. Geim, S.V. Morozov, D. Jiang, Y. Zhang, S.V. Dubonos, I.V. Grigorieva, A.A. Firsov, Electric field effect in atomically thin carbon films, *Science* 306 (2004) 666–669.
- [12] Y. Dan, Y. Lu, N.J. Kybert, Z. Luo, A.T.C. Johnson, I.V. Grigorieva, A.A. Firsov, Intrinsic response of graphene vapor sensors, *Nano Lett.* 9 (2009) 1472–1475.
- [13] G. Lu, L. Ocola, J. Chen, Gas detection using low-temperature reduced graphene oxide sheets, *Appl. Phys. Lett.* 94 (2009) 083111.
- [14] G. Lu, L. Ocola, J. Chen, Reduced graphene oxide for room-temperature gas sensors, *Nanotechnology* 20 (2009) 445502.
- [15] H.Y. Jeong, J.Y. Kim, J.W. Kim, J.O. Hwang, J.E. Kim, J.Y. Lee, T.H. Yoon, B.J. Cho, S.O. Kim, R.S. Ruoff, S.Y. Choi, Graphene oxide thin films for flexible nonvolatile memory applications, *Nano Lett.* 10 (2010) 4381–4386.

- [16] T. Kim, Y. Gao, O. Acton, H. Yip, H. Ma, H.Z. Chen, A.K. Jen, Graphene oxide nanosheets based organic field effect transistor for nonvolatile memory applications, *Appl. Phys. Lett.* 97 (2010) 023310.
- [17] L.M. Li, Z.F. Du, S. Liu, Q.Y. Hao, Y.G. Wang, Q.H. Li, T.H. Wang, A novel nonenzymatic hydrogen peroxide sensor based on  $\text{MnO}_2$ /graphene oxide nanocomposite, *Talanta* 82 (2010) 1637–1641.
- [18] N. Medhekar, A. Ramasubramaniam, R.S. Ruoff, V. Shenoy, Hydrogen bond networks in graphene oxide composite paper: structure and mechanical properties, *ACS Nano* 4 (2010) 2300–2306.
- [19] M. Acik, C. Mattevi, C. Gong, G. Lee, K. Cho, M. Chhowalla, Y. Chabal, The role of intercalated water in multilayered graphene oxide, *ACS Nano* 4 (2010) 5861–5868.
- [20] F. Barroso-Bujans, S. Cervený, A. Alegría, J. Colmenero, Sorption and desorption behavior of water and organic solvents from graphite oxide, *Carbon* 48 (2010) 3277–3286.
- [21] S. Park, J. An, J. Suk, R.S. Ruoff, Graphene-based actuators, *Small* 6 (2010) 210–212.
- [22] W.S. Hummers, R. Offeman Jr., Preparation of graphitic oxide, *J. Am. Chem. Soc.* 80 (1958) 1339.
- [23] M. Zimmermann, T. Volden, K. Kirstein, S. Hafizovic, J. Lichtenberg, A. Hierlemann, A CMOS-based sensor array system for chemical and biochemical applications, in: *Proceedings of the 31st European Solid-State Circuits Conference*, Grenoble, France, IEEE, Washington, DC, 2005, pp. 343–346.
- [24] S. Stankovich, R.D. Piner, S.T. Nguyen, R.S. Ruoff, Synthesis and exfoliation of isocyanate-treated graphene oxide nanoplatelets, *Carbon* 44 (2006) 3342–3347.
- [25] A. Lerf, A. Buchsteiner, B. Pieper, S. Schöttl, I. Dekany, T. Szabo, H.P. Boehm, Hydration behavior and dynamics of water molecules in graphite oxide, *J. Phys. Chem. Solids* 67 (2006) 1106–1110.

## Biographies

**Yao Yao** was born in Sichuan, China, in 1983. He received his BS degree from the School of Information Science and Technology, Southwest Jiaotong University, Sichuan, China in 2006. He is currently pursuing his PhD degree at the Southwest Jiaotong University, Sichuan, China. His current research interests include frequency control and acoustic wave sensor for environmental detection.

**Xiangdong Chen** was born in Jiangxi, China, in 1967. He received the PhD degree from University of Electronic Science and Technology, Sichuan, China in 1999. He is currently a Professor in the School of Information Science and Technology, Southwest Jiaotong University, Sichuan, China. He is the author or coauthor of more than 90 research papers. His current research interests include sensor technology, signal processing, and piezoelectric devices.

**Huihui Guo** was born in Henan, China, in 1983. He is presently working on the PhD degree in the School of Information Science and Technology, Southwest Jiaotong University, Sichuan, China. His current research interests include MEMS sensor and acquisition of intelligent information.

**Zuquan Wu** was born in Sichuan, China, in 1982. He is presently working on the PhD degree in the School of Information Science and Technology, Southwest Jiaotong University, Sichuan, China. His current research interests include sensor and conducting thin film.

**Xiaoyu Li** was born in Sichuan, China. She is presently working on the PhD degree in the School of Information Science and Technology, Southwest Jiaotong University, Sichuan, China. Her current research interests include gas sensor.